AD-A173 211 A STUDY OF FATIGUE CRACK PROPAGATION IN POWDER METALLURGY HOT ISOTATICALL..(U) LEHIGH UNIV BETHLEHEM PA DEPT OF METALLURGY AND MATERIALS ENG.. 1/1

UNCLASSIFIED R W HERTZBERG 28 AUG 86 AFOSR-TR-86-0920 F/G 11/6 NL

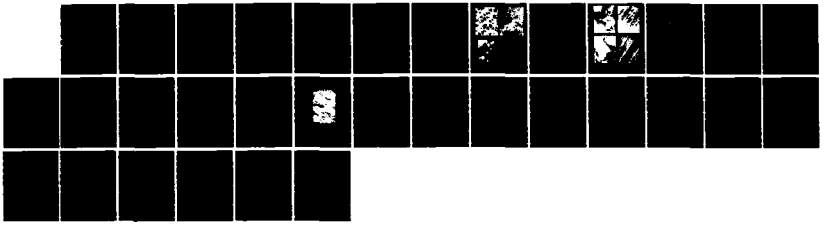

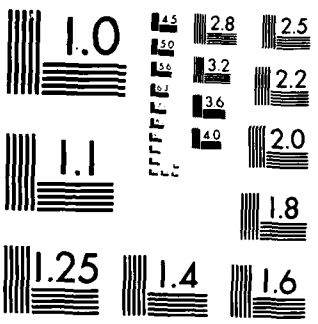

MICROCOPY RESOLUTION TEST CHART
NATIONAL BUREAU OF STANDARDS 1963-A

AFOSR-TR- 86-0920

A STUDY OF FATIGUE CRACK PROPAGATION IN POWDER METALLURGY HOT ISOTATICALLY PRESSED NICKEL-BASE ALLOY

AFOSR-83-0029
FINAL REPORT - AUGUST 1986

R. W. Hertzberg

Approved for public release;
distribution unlimited.

DTIC
ELECTE
OCT 16 1986
A

AD-A173 211

DTIC FILE COPY

Abstract

L.C. Astroloy contains a complex distribution of rounded cuboidal γ' precipitates (0.1 μm edge dimension), cooling γ' (0.01 μm dia) and prior particle boundary particles of MC, ZrO_2, α-Al_2O_3 and M_3B_2; the majority of MC carbides were not found in conjunction with ZrO_2 particles as was previously assumed.

ΔK_{th} values were found to vary with specimen geometry with lower values being associated with more symmetrical specimen geometries. With four-point bend samples, ΔK_{th} increased with increasing grain size, in agreement with previous findings.

The present work has identified several anomalies which exist with respect to crack closure measurements and their correlation of FCP rates. Closure values differed markedly in repeated K-decreasing threshold determinations even though fatigue crack growth rates remained unchanged. The introduction of an artificial asperity in the wake of the crack tip in a 2024 aluminum alloy gave rise to large measured values of closure which had little influence on the crack growth rates; apparently, crack closure had little influence on associated crack growth rates.

Based on experimental and analytical work LEFM principles break down in the "so-called anomalous" short crack regime at relatively high σ/σ_{ys} ratios (e.g., $\sigma/\sigma_{ys} > 0.5$). For example, a fractographic analysis of both long and short crack length specimens revealed different micromechanisms and dissimilar development of shear lips at the same computed ΔK levels. Analytical results also indicated that correlation of short crack data in terms of ΔK is suspect since the near field crack tip stress-strain fields do not possess the required $1/\sqrt{r}$ singularity necessary for the application of LEFM. Short crack data only appear anomalous when plotted in terms of ΔK. However, when short crack and long crack data are analyzed in terms of the strain energy density criterion, excellent agreement is obtained. In addition, this driving force parameter can also account for mean stress effects and rationalize differences in the macroscopic and microscopic fractographic features of long and short cracks.

86 10 16 145

PROGRAM OBJECTIVES

The overall objective of this program was to characterize the fatigue crack propagation (FCP) behavior of powder metallurgy (PM)-hot isostatically pressed (HIP'd) Astroloy nickel based alloy. The findings of this research are particularly relevant to the proper design of gas turbine engine components, such as the turbine disk. Material, environment, load history and specimen geometry variables were examined as follows:

Material variables: It has been shown that microstructural variations in grain size and precipitate morphology can affect FCP rates when assessed according to linear elastic fracture mechanics (LEFM) principles. Although these parameters are often difficult to control, the advent of powder metallurgy (P/M) processes have facilitated the development of alloys in which control of grain size and precipitate distribution may be realized without the possible detrimental influences of segregation effects. Accordingly, a study of the effects of grain size and γ' precipitate distribution on FCP response and localized crack tip deformation mechanisms was undertaken at both room temperature and 650°C in association with various test frequencies and load ratios. The role of grain size on FCP resistance is of particular interest in light of recent findings which show improved cracking resistance with increased grain size (e.g., Ref. 1-4).

Despite the obvious attractions of PM techniques some problems may be associated with its use in highly alloyed systems such as nickel based superalloys. In addition to the problems associated with inherent porosity, detrimental mechanical properties may result from the undesirable nature of the precipitation on the original powder particle boundaries (PPBs) (5-6). The precipitates may restrict grain growth of the material thus limiting the development of large grained materials; secondly, they cause a reduction in the amount of specific elements available for the precipitation of beneficial phases; and thirdly, the PPB precipitates themselves may be brittle and thus provide an easy fracture path. The nature of the precipitates and possible methods of controlling the precipitation behavior are therefore of importance. Therefore, an objective of the present work was to investigate the nature of the second phase particles present in a PM HIP'd nickel base superalloy. To this end, detection methods based on the generation of x-ray spectra are limited either in terms of the elemental

A-1

detection capabilities or, in the case of EELS, in terms of the required specimen thickness (7). A more efficient and direct guide to the precipitates crystal structure and its related composition has been obtained by considering the nature of the diffraction from individual second phase particles. In addition, the influence of various heat treatments after powder compaction on the incidence and distribution of the PPB precipitates was also investigated.

Influence of crack length: Recent studies (8-12) have shown that the absolute length of the fatigue crack can have a pronounced effect on FCP rates. The growth characteristics of short cracks, whose depth and length dimensions are generally less than 1-2 mm, have generated concern in the design community because of their "apparent anomalous" behavior when assessed according to LEFM principles; it is not uncommon to observe up to an order of magnitude or more higher FCP rates for short cracks when compared with FCP rates determined from long crack samples evaluated at the same ΔK level. In addition, short cracks can also propagate at ΔK levels below the so-called long crack threshold.

Because of the "apparent" anomalous behavior of short fatigue cracks when correlated in terms of the stress intensity range, it was important to identify whether differences in failure micro-mechanisms are responsible for this anomalous behavior. To this end, the effect of various microstructural conditions on short fatigue crack growth were studied. In addition, it was equally important to characterize the growth behavior of these short cracks in terms of an alternative driving force parameter. For example, the anomalous behavior of short cracks when their associated FCP rates are correlated in terms of the stress intensity range, reflects the fact that the stress and strain distributions ahead of the crack tip do not possess the $1/\sqrt{r}$ singularity presumed to exist for cases involving linear elastic behavior. To this end, the applicability of the strain energy density criterion to short fatigue crack growth was examined since this criterion may predict more realistic deformation fields.

Influence of specimen geometry on FCP response: It has long been assumed that FCP rates for a given material are similar for a given ΔK level, regardless of specimen geometry. Recently, however, Fine and co-workers (13,14) reported that the threshold behavior of HY80 and type 1018

steels varied with specimen geometry; lower ΔK_{th} values were recorded with symmetrically loaded center-cracked tension specimens as compared with values obtained from asymmetrically loaded single edge-notched specimens. Since component life prediction depends strongly on threshold stress intensity values, it was considered necessary to examine the threshold response of Astroloy as a function of specimen geometry. Consideration of the observed discrepancies was given in terms of crack closure levels behind the crack tip and the stress distribution and deformation behavior of the material affecting crack advance.

Applicability of crack closure measurements to the analysis of FCP behavior: Crack closure is considered by some to be an important parameter when describing crack growth in Region I (15,16). Generally, closure arguments are used to explain the observed threshold behavior in many materials and also used to normalize the effects of load ratio (mean stress level) on crack growth behavior. From a design standpoint, it is important to examine the usefulness and applicability of crack closure information with regard to the prediction of FCP rates in a structural component and to consider, if needed, the development of alternative correlation parameters. A major objective of this report was to identify some areas of concern regarding the measurement of closure and its significance in analyzing FCP data. Also, the intention will be to examine the significance of crack closure generated in conjunction with ΔK-decreasing test procedures associated with FCP threshold determination.

Variable amplitude loading: Since most structures experience loads of varying magnitude rather than constant amplitude, it was deemed important to characterize the fatigue crack growth response of a component under random loading conditions. To this end, the effect of 50% tensile overloads (typical in gas turbine disks) on the subsequent fatigue crack growth (at 24°C) was studied in terms of the base line stress intensity level and the material's microstructural condition.

EXPERIMENTAL FINDINGS AND CONCLUSIONS

Material Characterization: Low Carbon (L.C.) Astroloy a powder metallurgy (P/M), hot isostatically pressed (HIP'd) Ni-base superalloy was used in the present investigation. The composition of the alloy is given in Table I. Samples with differing grain sizes (5-50 μm) were produced by altering the HIP and solution treatment procedures. Thermal treatments used in this study are given in Table II along with material properties and specimen designations. The L.C. Astroloy contains a complex distribution of second phase particles. Studies revealed a distribution of rounded cuboidal γ' precipitates of approximately 0.1 μm edge dimension together with some γ' of approximately 0.01 μm diameter (Fig. 1a). Second phase particles associated with the original powder particle boundaries were also observed (Fig. 1b). These individual particles have been identified using energy dispersive x-ray analysis and convergent beam electron diffraction. Four distinct types of particles have been observed: a cubic MC carbide in which M is either titanium or titanium plus molybdenum, a monoclinic phase ZrO_2, a trigonal α-Al_2O_3 and a tetragonal M_3B_2 phase in which M is molybdenum or molybdenum and chromium. The observations indicate that, although some MC carbides are associated with the ZrO_2 phase, the majority of the prior particle boundary precipitates are separate entities (Fig. 1c). HIP'ing or subsequent heat treatments above or below the γ' solvus were observed to have little effect on the incidence or distribution of the precipitation associated with the prior particle boundaries. In contrast, heat treatments above the γ' solvus resulted in the dissolution of the M_3B_2 phase and its preferential precipitation on the grain boundaries. (For further details, see Publications - Manuscript No. 5.)

To characterize the dislocation structure of L.C. Astroloy after cyclic loading at 650°C, unnotched samples were cycled under load control at a load ratio of 0.1 and at frequencies of 30 and 0.3 Hz. Specimens with grain sizes of 5 and 26 μm were sectioned perpendicular to the loading axis and near to the fracture surface with thin films prepared for viewing in the TEM.

The influence of grain size on the dislocation structure did not result in a straightforward relationship since the observations depend on the frequency of testing. At 30 Hz the 5 μm grain sized material showed a low

Table I. Composition of HIP'd L.C. Astroloy (wt.%)

Co: 16.98; Cr: 14.80; Mo: 5.07; Al: 3.99; Ti: 3.58;

Fe: 0.21; Zr: 0.047; B: 0.026; C: 0.024; Si: 0.02;

Mn: 0.01; Cu: 0.01; W: 0.01; P: 0.003; N: 0.002;

S: 0.001; Ni balance

Table II. Specimen Thermal Treatments, Material Properties and Designations

Spec.* No.	H.I.P. 2h	Solution+ Treatment 2h	Age 24h	Grain Size	Yield Stress (MPa)	U.T.S. (MPa)
1A,B	1107°C	1121°C	650°C	5 μm	1110	1550
2A,B	1107°C	1149°C	650°C	13 μm	1070	1460
3A,B	1107°C	1177°C	650°C	26 μm	965	1400
4A,B	1246°C	1149°C	650°C	50 μm	910	1350

*Note: A's correspond to specimens tested at room temperature while B's correspond to specimens tested at 650°C.

+The γ' solvus was found to be in the temperature range of 1130-1140°C.

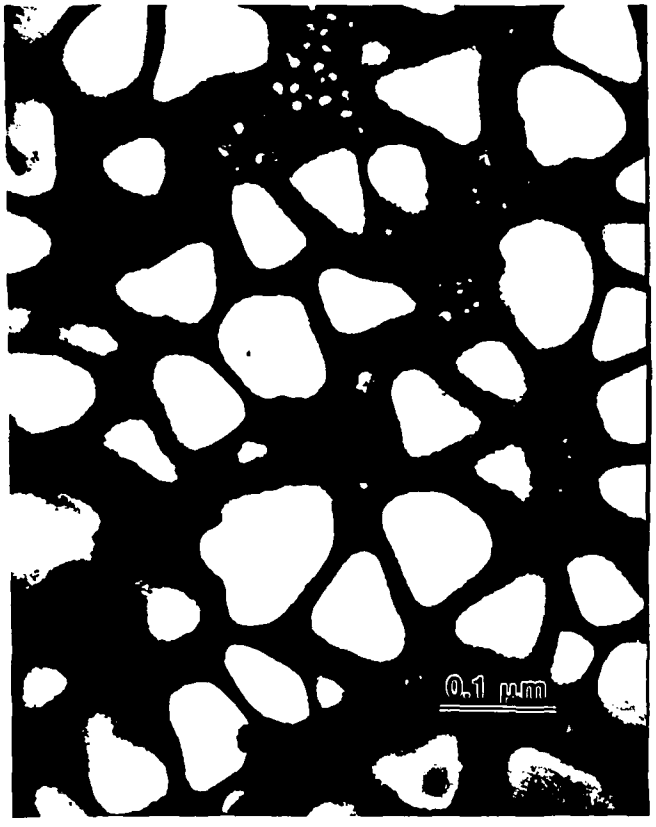

a

b

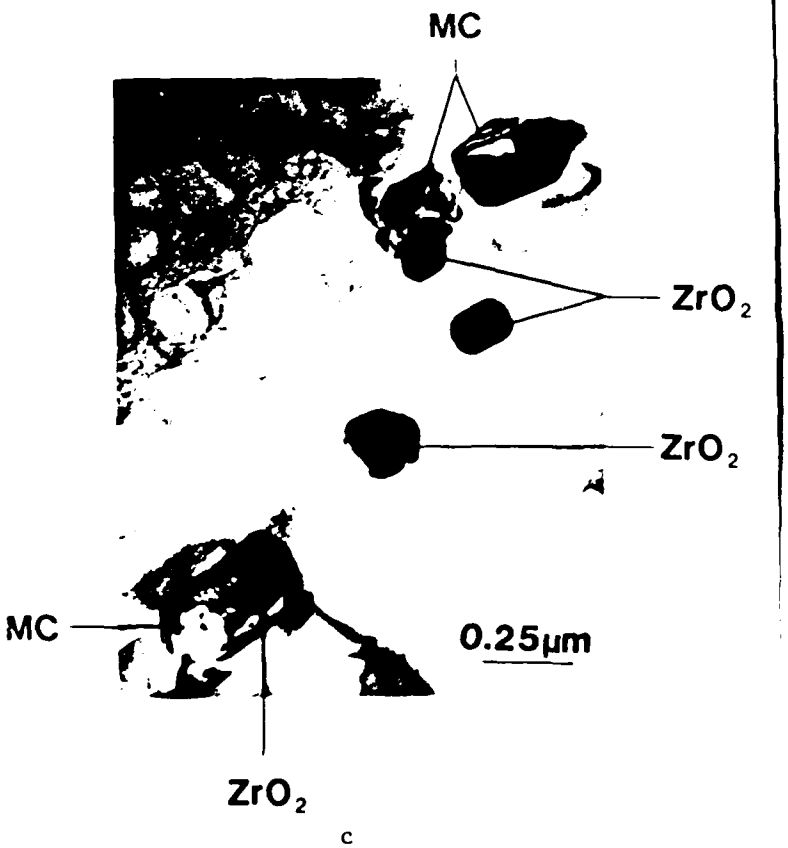

c

Fig. 1. Microstructure of L.C. Astroloy. a) γ' precipitate size distribution; b) precipitates on prior particle boundaries of three powder particles; c) MC and ZrO_2 particles on PPB. In most cases, the phases are separate.

dislocation density with an inhomogeneous dislocation structure evident (Fig. 2a). Dislocations were generally confined to narrow slip bands with few slip bands per grain. At the same frequency, the 26 μm grain size material revealed a similarly inhomogeneous dislocation structure but with a much higher dislocation density (Fig. 2b). At 0.3 Hz the observations differed. For the 5 μm grain size a high density fine homogeneous dislocation structure was evident (Fig. 2c) whereas the 26 μm grain size material showed the same inhomogeneous dislocation structure with a high dislocation density within the slip bands (Fig. 2d).

What is puzzling is the sensitivity of the dislocation structure in the 5 μm grain sized material to changes in frequency. With a 100 fold decrease in the frequency, there is a drastic change in the dislocation structure from inhomogeneous with a low dislocation density to homogeneous with a high dislocation density. In contrast, the 26 μm grain sized material shows little change in dislocation structure with changing frequency.

Despite the differences in dislocation structure between these conditions of either material or deformation, the only anomally in terms of measured failure life was obtained on the 30 Hz test on the 26 μm material. All the other tests showed lifetimes of approximately 2×10^5 whereas the 30 Hz, 26 μm test gave a lifetime of $\cong 1 \times 10^4$ cycles. This anomally cannot be simply rationalized in terms of the dislocation structures observed.

While the dislocation structure may be a unique combination of material parameters and testing condition it is by no means established that a particular dislocation structure is associated with a certain failure lifetime. Hence a complete understanding of the behavior must reflect the influence of testing variables such as temperature and frequency as well as considering the material variables such as grain size and precipitate structure. At present the results of this study do not provide a clear understanding of this relationship and in particular do not provide a clear and unambiguous understanding of the relationship to the specimen lifetime. Additional studies are indicated.

Fatigue Crack Propagation--Long Crack Samples: The results of the fatigue crack propagation tests using DC(T) specimens for the four microstructural conditions examined in this study are shown in Figure 3. At R = 0.1 (Fig. 3a) threshold stress intensity values are observed to be relatively

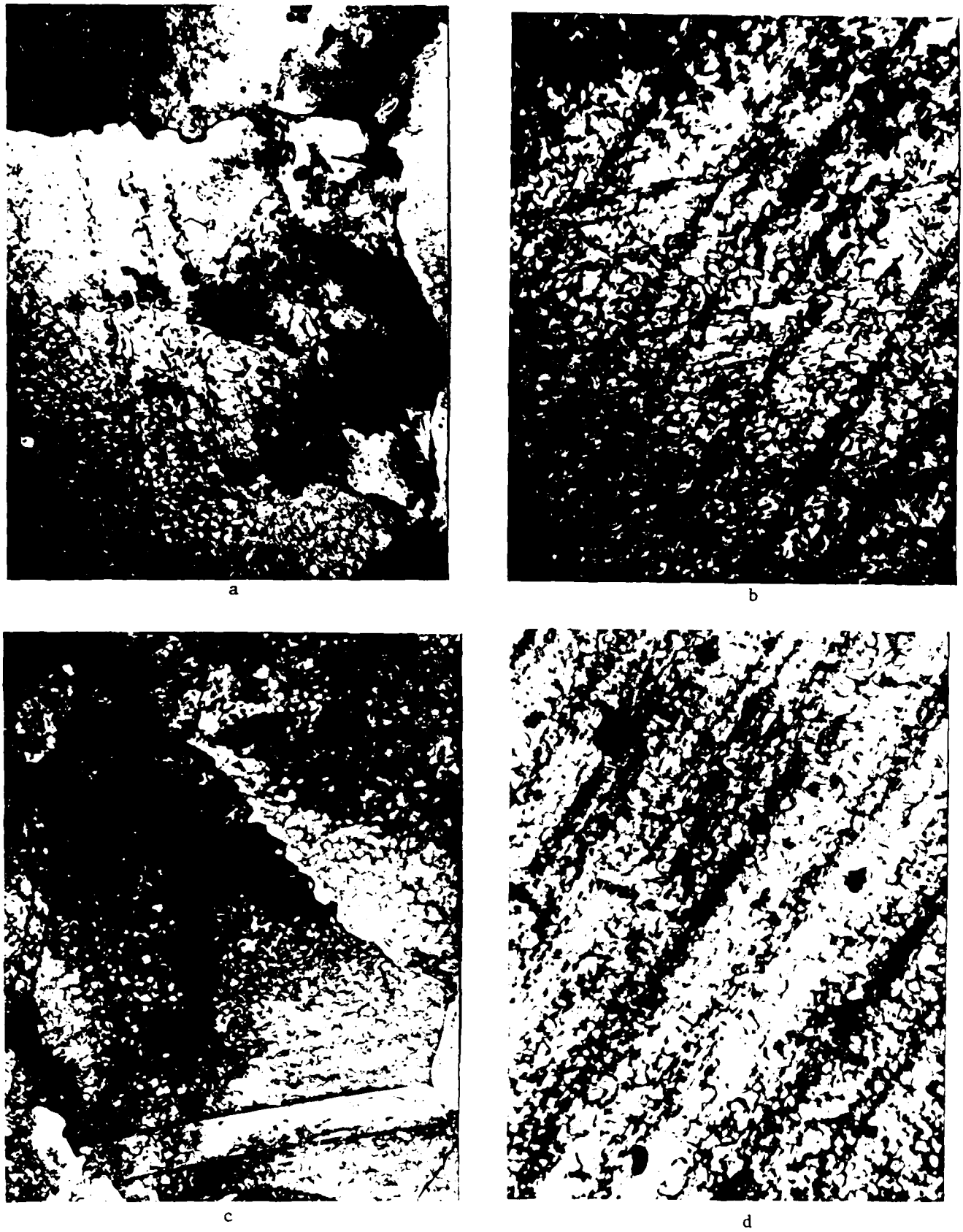

Fig. 2. Dislocation substructure in L.C. Astroloy from loading cycling at 650°C, 11,000X. a) 5 μm grain size, 30 Hz, $N_f \approx 2 \times 10^5$; b) 26 μm grain size, 30 Hz, $N_f \approx 10^4$; c) 5 μm grain size, 0.3 Hz, $N_f \approx 10^3$; and d) 26 μm grain size, 0.3 Hz, $N_f \approx 2 \times 10^5$.

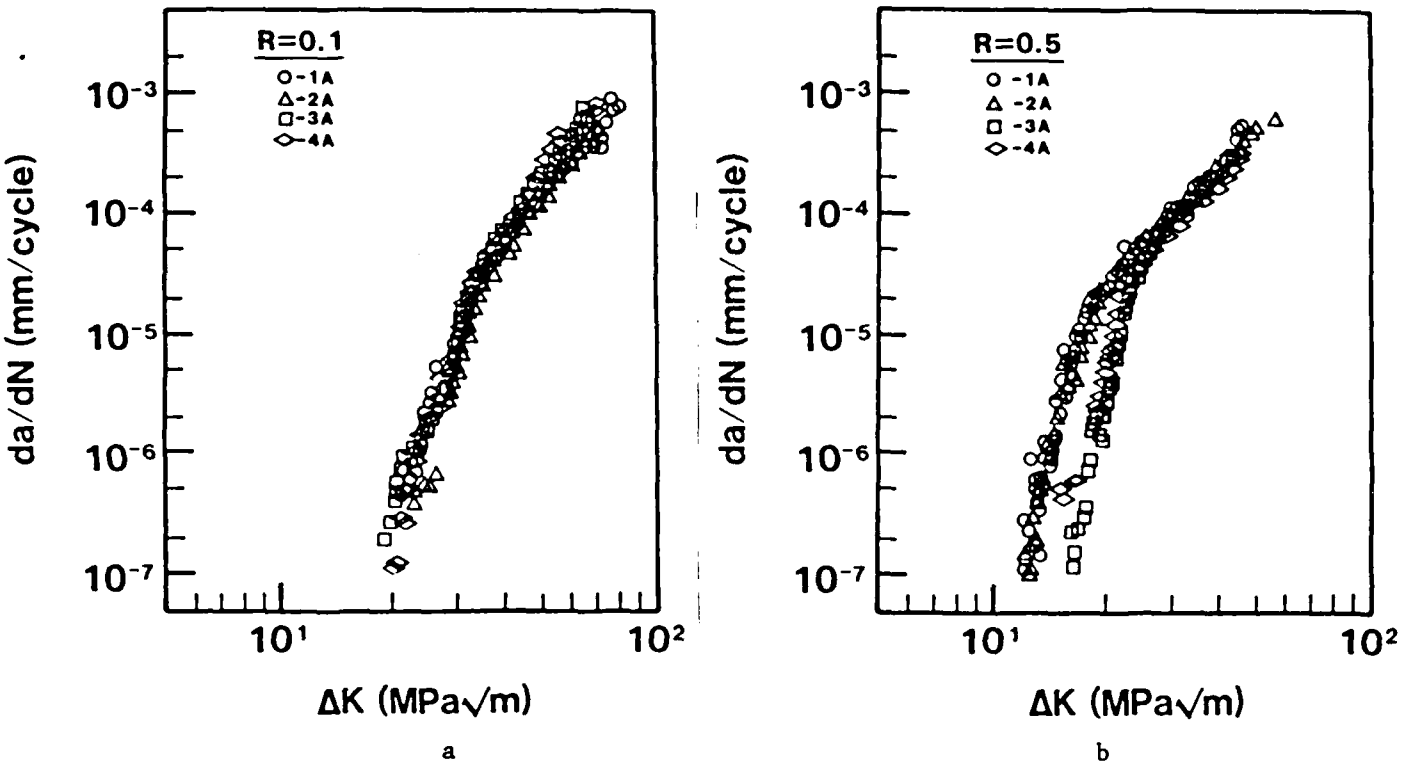

Fig. 3. Effect of grain size on FCP response of Astroloy for DC(T) samples. Grain sizes are: 1A-5 μm, 2A-13 μm, 3A-26 μm and 4A-50 μm. a) R = 0.1; b) R = 0.5.

insensitive to changes in grain size. However, as shown in Figure 3b, increasing R to 0.5 reveals a grain size dependence on ΔK_{th}; increasing grain size yields higher threshold stress intensity levels. A comparison of these results with those obtained by King et al. (17) for L.C. Astroloy indicates that ΔK_{th} values obtained in this study are approximately two times higher than those found by King et al. (17). In addition, the latter results showed a grain size dependence at both R ratios of 0.1 and 0.5. At higher crack growth rates in Region II, however, good agreement between the results of this study with those in (17) was obtained. A comparison of test procedures between this work and that of King and co-workers reveals that the only significant difference was in the specimen geometries used. Additional threshold tests were, therefore, conducted using the four point bend (4PTB) geometry similar to the three point bend (3PTB) geometry used by King et al.

The near threshold FCP response of Astroloy evaluated with the 4PTB configuration (R = 0.1) for grain sizes of 5, 26, and 50 μm is presented in Figure 4. Also shown in this figure are DC(T) FCP results from the 5 and 50 μm grain size materials and the bend bar results from King (17). It is clear from Figure 4 that there is good agreement between the 4PTB threshold results of this study and the 3PTB threshold results of King (17). In addition, a similar dependence of threshold stress intensity levels on grain size is observed in both studies. Of greater significance, however, is the apparent dependence of ΔK_{th} values on specimen configuration; the crack growth rates in the threshold regime for the DC(T) samples are considerably lower than results obtained with the 4PTB configuration.

For a given value of ΔK in region I, crack growth rates were observed to increase as the specimen loading became more symmetrical with respect to the load line. As such, the DC(T) specimen exhibited lower growth rates than the more symmetrically loaded CCT specimen. This dependence is believed to be related to the interaction of the crack tip stress fields of the various specimen configurations with the material's microstructure. Elastic stress analysis by the finite element method revealed that for a given ΔK level, the CCT specimen possesses higher near crack tip Y-direction stresses than the CT specimen, Figure 5. As a result, the damage zone in the CT sample is smaller than that found in the CCT specimen at the same applied ΔK level. It is therefore suggested that microstructural domination

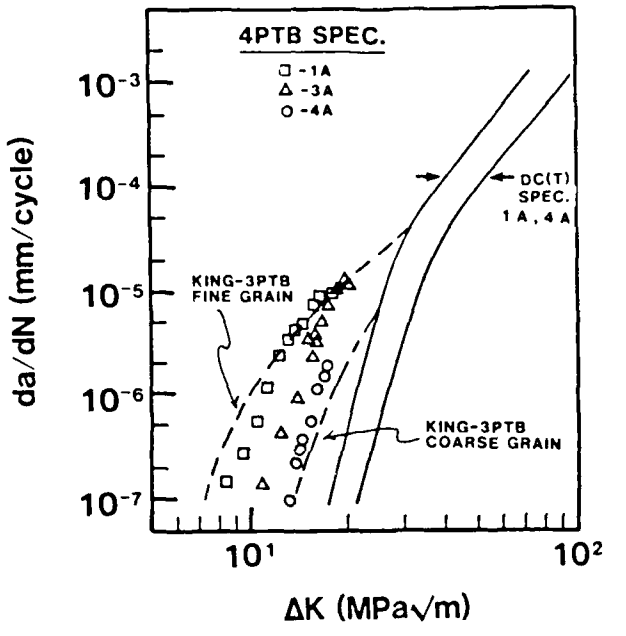

Fig. 4. Comparison of FCP rate results between DC(T) and 4 point bend (4PTB) samples and 3PTB results from Ref. 17. Grain sizes are: 1A-5 μm, 2A-13 μm, 3A-26 μm and 4A-50 μm.

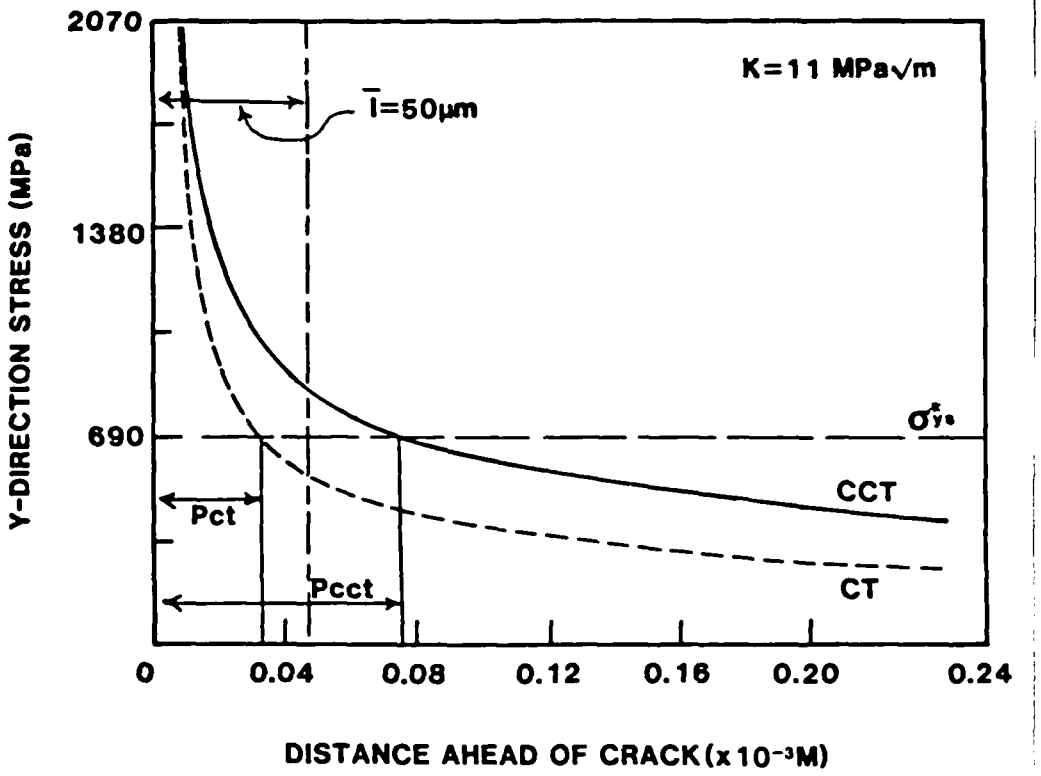

Fig. 5. Effect of differing near field stress distributions on the process zone sizes, P, ahead of a crack for the CT and CCT specimens.

of crack growth will occur at higher ΔK levels for the CT specimen as compared to the CCT specimen. (For further details, see Publications - Manuscripts 1 and 8.)

The fatigue crack propagation response of Astroloy at 650°C and at a cyclic frequency of 30 Hz is summarized in Figure 6 for R ratios of 0.1 and 0.5. It is clear that increasing temperature from 24°C to 650°C significantly increases the crack propagation rate at a given ΔK level. Although the growth rates measured in this temperature regime do not correspond to threshold conditions, an increase in the gradient of the da/dN-ΔK curves does occur with decreasing ΔK levels. It is worth noting, however, that the results for R = 0.1 indicate that if the 650°C FCP tests were continued to lower ΔK levels, ΔK_{th} would be similar to the room temperature ΔK_{th} values. This trend is in agreement with those reported by Hicks and King for a similar material (18). It is also apparent from these results that at low to intermediate stress intensity values, there is a significant influence of stress ratio on the crack growth rate. At high ΔK levels, however, the influence of stress ratio diminishes. Little influence of grain size on the FCP behavior of this material was revealed at either stress ratio. (For further details pertaining to frequency influences and fracture surface appearance for high temperature tests, see Publications - Manuscript 10.)

An examination of the fracture surfaces in the different specimen geometries revealed similar characteristics. In region II, both 4PTB and DC(T) specimens revealed relatively smooth fracture surfaces covered with fatigue striations. As the applied ΔK level was reduced from region II to region I, the fracture surface revealed highly angular crystallographic facets with larger facets found in the larger grained material. Although this transition in fracture surface morphology occurs in all the specimen geometries examined here, the ΔK level at which this transition occurred varied with specimen configuration. In the DC(T) specimens the transitional ΔK level was higher than that found in the bend geometries.

Fatigue Crack Propagation--Short Crack Samples: Bend specimens containing short cracks (<300 μm) were machined from DC(T) samples and fatigue tested. The crack growth rate results for the short crack configuration indicate a dependence on both material properties and grain size, and the ratio of the

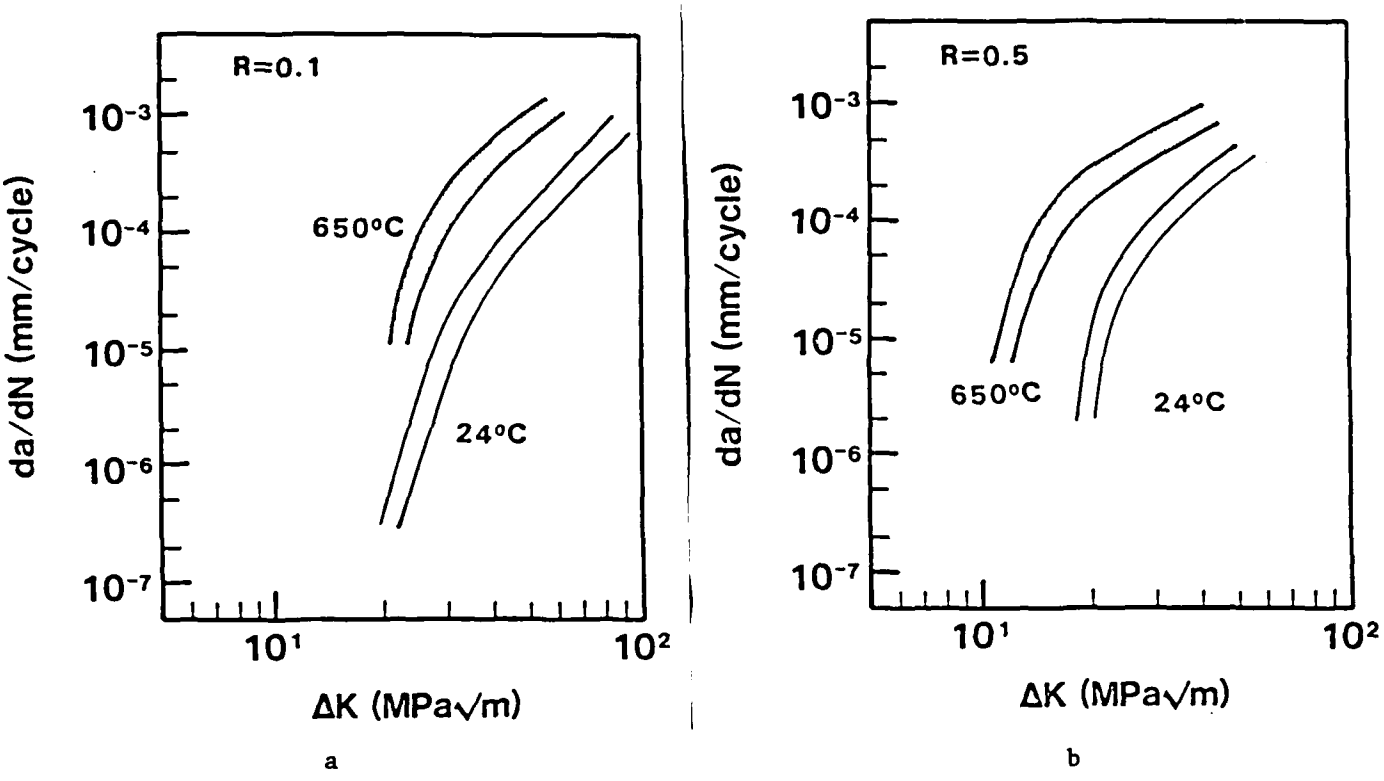

Fig. 6. Effect of temperature on the FCP behavior of Astroloy. Little influence of grain size is noted, a) R = 0.1; b) R = 0.5.

maximum applied stress to the yield stress (σ_m/σ_y) Figure 7a. As grain size is increased or yield strength decreased, crack growth rates decrease for a given value of ΔK. This difference in crack growth behavior increases for decreasing values of ΔK. In addition, Figure 7a also reveals that as σ_m/σ_y is increased for a given material, crack growth rates increase at high ΔK levels; as one would expect, this effect becomes more pronounced as ΔK approaches K_c.

When long and short crack FCP results are plotted together as a function of ΔK (Fig. 7b) the short cracks are seen to grow up to an order of magnitude or more faster than the long cracks. Such anomalous behavior of short cracks has been attributed to several different mechanisms (19-21). Here, however, it is suggested that this anomalous behavior is attributed to the improper use of LEFM principles, due to an inability in the stress intensity factor to correctly describe the magnitude of the crack tip stress-strain field for the case of short cracks. Based on experimental and analytical work (performed during this contract period), it is clear that LEFM principles break down in the "so-called" short crack regime at relatively high σ/σ_{ys} ratios (e.g., $\sigma/\sigma_{ys} > 0.5$). For example, a fractographic analysis of both long and short crack length specimens reveals different micromechanisms and dissimilar development of shear lips at the same computed ΔK levels, Figure 8. The lack of correspondence between macroscopic and microscopic fracture surface appearance in short and long crack samples can dramatically compromise commonly used failure analysis techniques in the interpretation of failed service components. Analytical results also indicate that correlation of short crack data in terms of ΔK is suspect since the near field crack tip stress-strain fields do not possess the required $1/\sqrt{r}$ singularity necessary for the application of LEFM. Short crack data only <u>appear</u> anomalous when plotted in terms of ΔK. However, when short crack and long crack data are analyzed in terms of the strain energy density criterion (22-24), excellent agreement is obtained (Fig. 9). In addition, this driving force parameter can also account for mean stress and temperature effects and rationalize differences in the macroscopic and microscopic fractographic features of long and short cracks. (For further details, see Publications - Manuscript No. 2.)

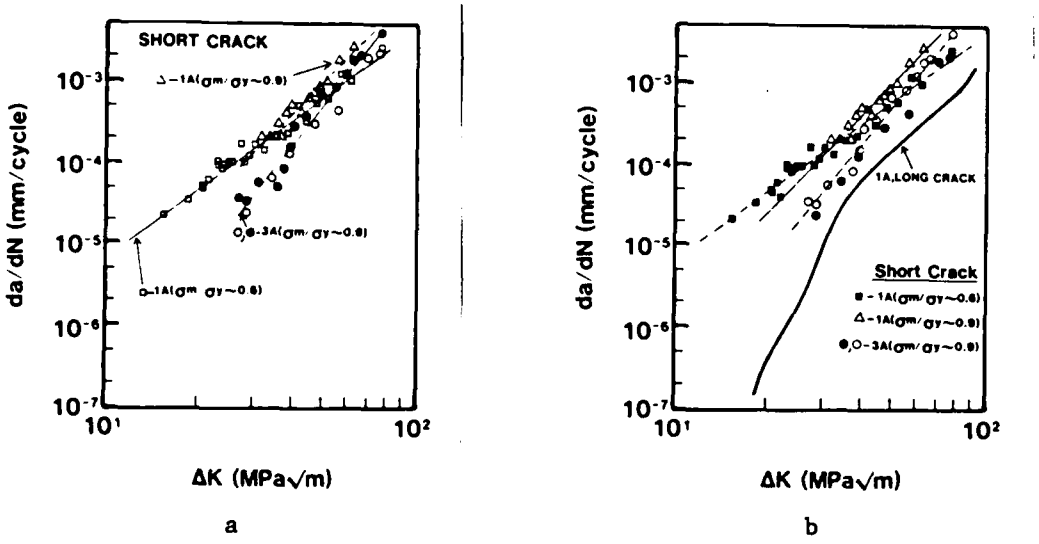

Fig. 7. Short crack FCP data in Astroloy as a function of ΔK. Grain size: 1A-5 μm, 3A-26 μm. a) short crack data; b) comparison of short and long crack growth rate data.

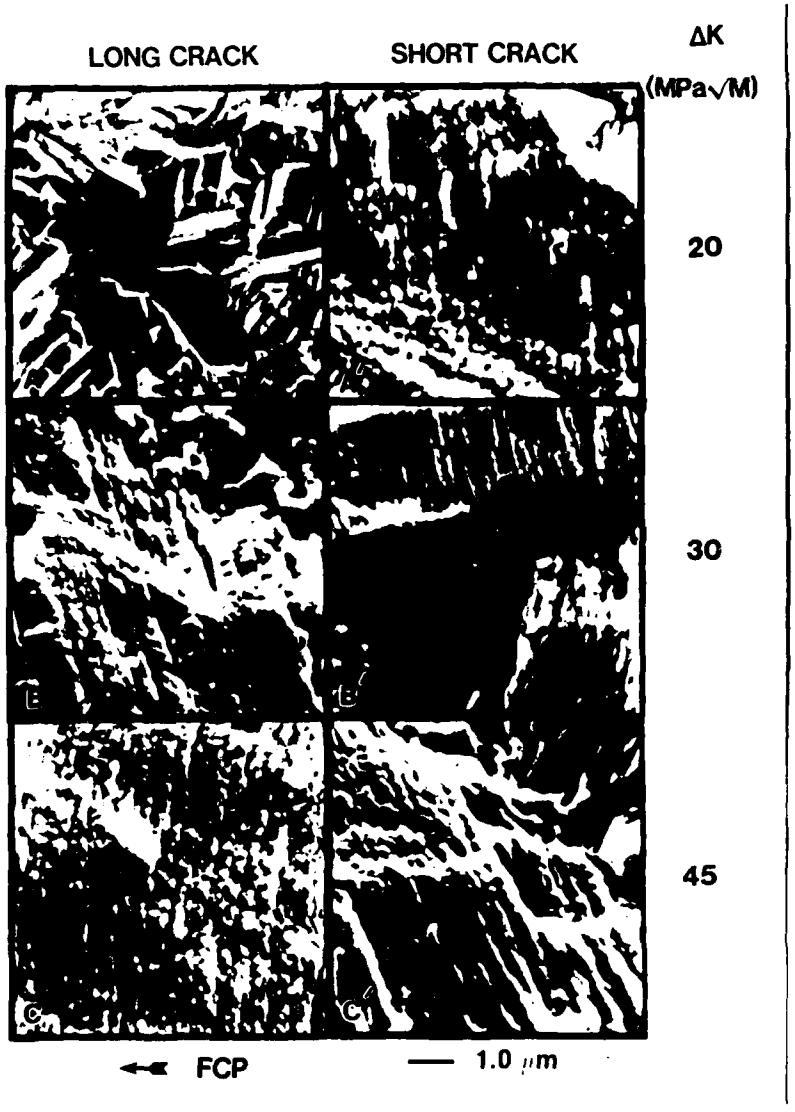

Fig. 8. Scanning electron micrographs of both long and short crack fracture surface morphologies at various ΔK levels (R = 0.1).

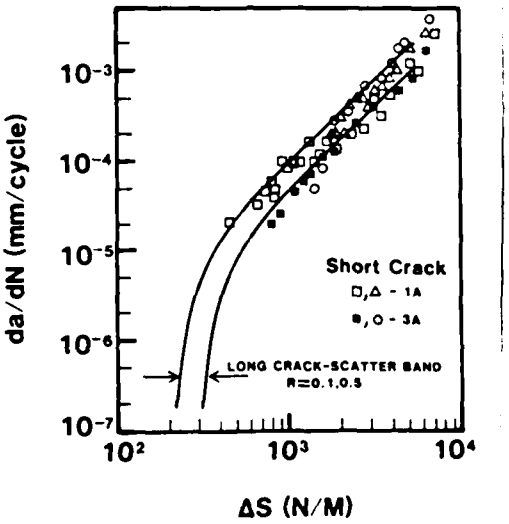

Fig. 9. Comparison of long and short FCP data as a function of ΔS. Note improvement over correlation with ΔK.

Applicability of Crack Closure Measurements to the Analysis of FCP Behavior: The rapid decrease in crack growth rates associated with decreasing ΔK levels (at low values of ΔK) is believed to be related to a significant decrease in the effective crack driving force that results from a pronounced increase in the level of crack tip closure (Fig. 10). If crack growth rates are correlated in terms of the effective cyclic stress intensity, ΔK_{eff} (Fig. 11), a normalization of the stress ratio influence on crack growth rates occurs in region II where Elber-type (25,26) closure mechanisms are believed to occur. However, in the near threshold regime (region I) where closure due to crack deflection and/or asperity interference is believed to dominate (16,27), significant scatter in crack growth rate data arises. Similar results have been reported previously by Stofanak et al. (28).

Additional evidence supporting the nonuniqueness of closure in region I is presented in Figure 12. Figure 12a reveals (for the 50 μm grain size material) significantly different crack closure values from two separate K-decreasing procedures performed on the same specimen. If crack closure truly influences near threshold behavior then one would expect to see very different crack growth rate behavior between these two tests when evaluated in terms of $\Delta K_{applied}$. As shown in Figure 12b however, the crack growth rate data are in excellent agreement. Similar results were obtained for the 26 μm grain size material. Identical FCP rate behavior with differing crack closure information suggests that such closure measurements do not reflect a material characterization as suggested in (16,27,29,30) but rather represent an artifact of the testing procedure (31,32) and/or specimen configuration.

The introduction of spurious asperity (i.e., a needle tip) into the wake of the crack tip enabled one to study the effect of known artifically induced levels of closure on the crack growth rate. Cracks were propagated at a constant baseline stress intensity (ΔK_b) in a 2024 aluminum alloy with 45-50% and 60-70% levels of closure being artifically introduced. The results of these tests indicate that the crack growth rate changed marginally despite a dramatic increase in apparent closure levels associated with the introduction of the spurious crack face asperities. Comparison of these FCP data with other data for 2024 aluminum, indicates that the observed crack growth rates were approximately an order of magnitude higher than would be expected from the level of ΔK_{eff} defined by the measured closure value.

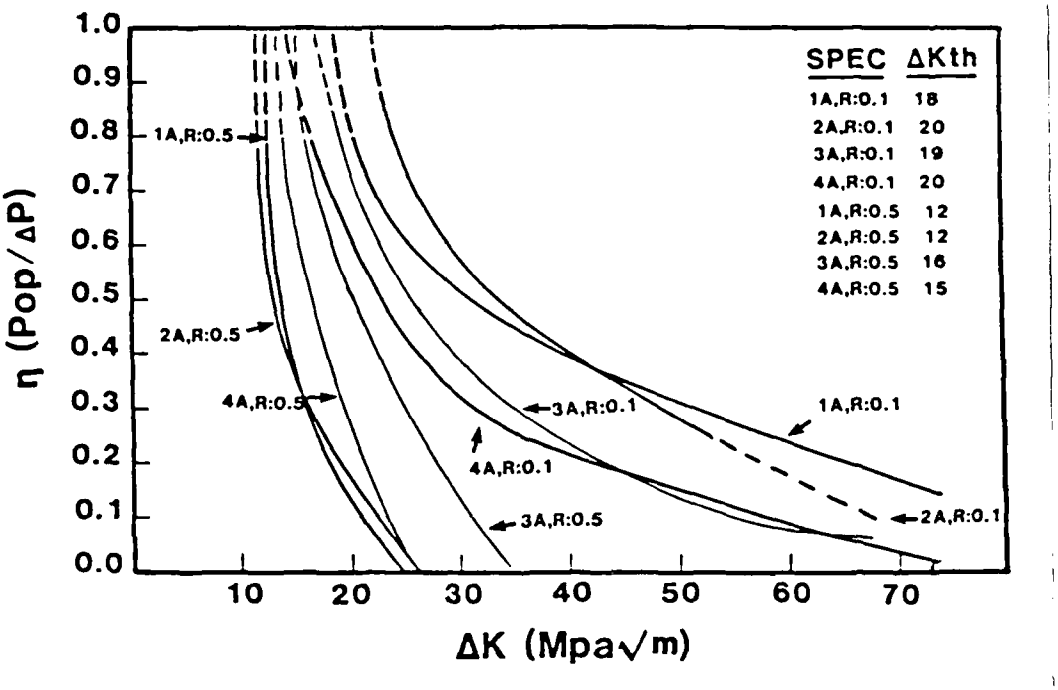

Fig. 10. Measured crack closure data for Astroloy DC(T) samples at room temperature.

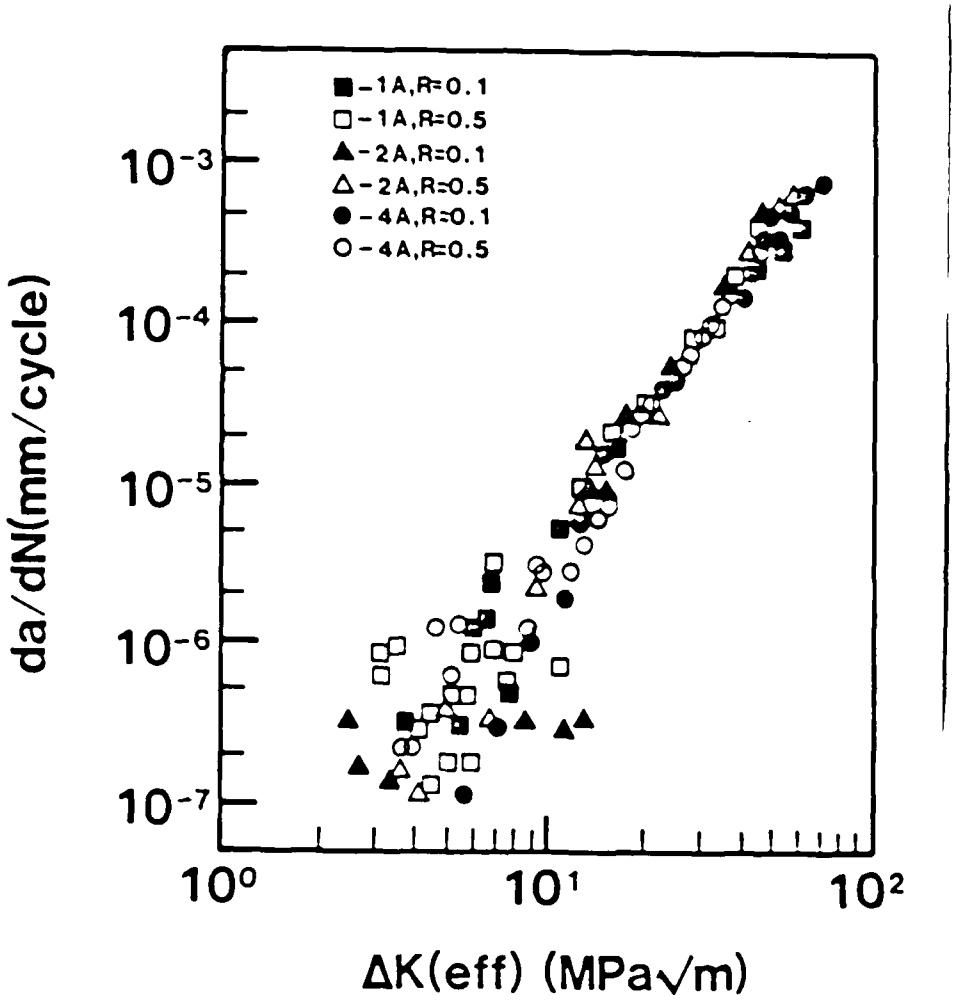

Fig. 11. Fatigue crack growth behavior of Astroloy correlated in terms of ΔK_{eff} (DC(T) sample).

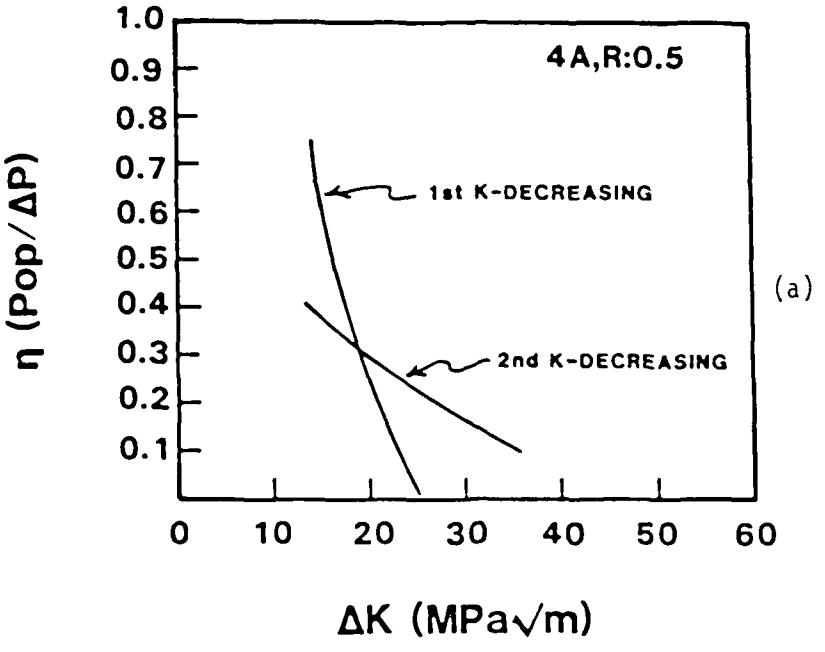

(a)

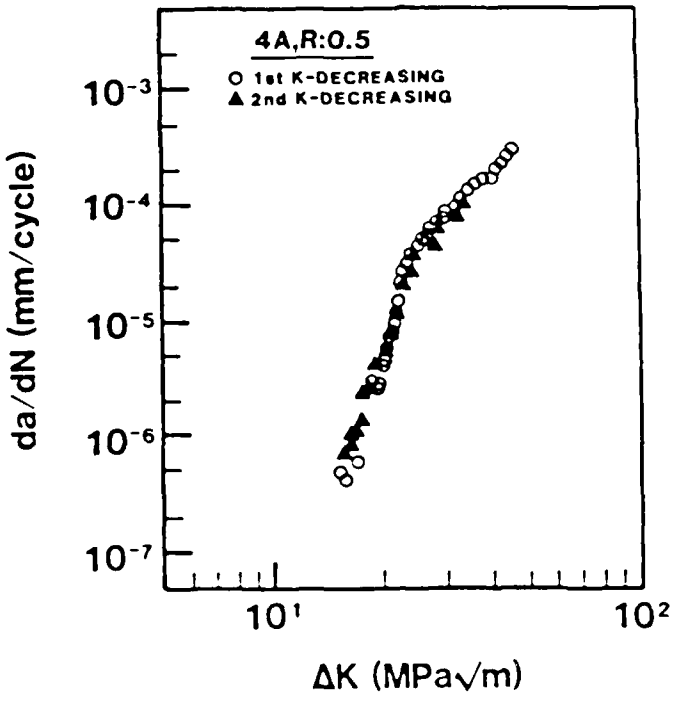

(b)

Fig. 12. a) Crack closure levels and b) FCP rates for two K-decreasing tests on the same specimen.

In the cases examined here, it is clear that the macroscopic crack closure level which has been measured bears little relation to the actual situation at the crack tip. Though it is recognized that the measurement of crack closure is sensitive to events in the wake of the crack tip, closure levels depend also on crack surface conditions remote from the crack tip. For this reason, incorporation of macroscopic crack closure measurements to the analysis of fatigue fracture processes at the crack tip appears controversial. Clearly more study is indicated. In addition, the K-decreasing procedure used to obtain ΔK_{th} is called into question in that it may produce an overestimate of a material's intrinsic FCP resistance through the development of excessive amounts of closure. Furthermore, it has been concluded that at least part of the difference between long and short crack propagation data may be traced to anomalously low FCP rates associated with long crack samples. (For further details, see Publications - Manuscripts 6 and 9.)

Variable Amplitude Loading: The effect of 50% single peak tensile overload cycles was determined for the Astroloy alloy for three different grain sizes (Table III). The large cyclic delays observed indicate that this material is extremely sensitive to the application of tensile overload cycles. The observed trend of decreasing cyclic delay with increasing ΔK_{base} is consistent with overload response associated with plane strain conditions (3,33-35). (For further details, see Publications - Manuscripts No. 1 and 10.)

Acknowledgements

The financial support by the U.S. Air Force under grant No. AFOSR-83-0029 is gratefully acknowledged along with the technical supervision of Dr. Alan Rosenstein, project monitor. The technical cooperation of Carpenter Technology, Reading, Pa. and I. M. T. Corp. Andover, Mass. in preparing and processing the Astroloy samples is appreciated.

TABLE III. Number of Cycles of Delay Due to 50% Tensile Overloads in L.C. Astroloy

ΔK_b (MPa$\sqrt{m}$)	Specimen Grain Size (μm)		
	5	26	50
30	150,000	140,000	350,000
35	42,000	43,000	30,000
40	19,000	18,000	16,000
45	9,500	8,000	11,000
50	6,500	5,000	5,500

REFERENCES

1. G. R. Yoder, L. A. Cooley, and T. W. Crooker, Eng. Fract. Mech., 11 p. 805 (1979).

2. J. Bartos and S. D. Antolovich, Fracture 1977, 2, ICF4, Waterloo, Canada, p. 995 (1977).

3. S. D. Antolovich, and N. Jayaraman, N., Fatigue, Environment and Temperature, J. J. Burke and V. Weiss, eds., Plenum Press, New York, p. 119 (1983).

4. J. E. King, R. A. Venables and M. A. Hicks, ICF6, India, Dec. 1984.

5. N. M. Allen, R. L. Athey and J. B. Moore, "Progress in Powder Metallurgy," G. D. Smith, ed., 31, Metal Powder Industries Federation, Princeton, NJ, p. 243 (1975).

6. J. Bressers, M. Roth, E. Fenske and P. Tambuyser, Proc. Int. Symp. on High Temp. Mat. for Gas Turbines, P. Contsouradis, ed., Liege, Belgium, p. 597 (1982).

7. D. B. Williams, Practical Analytical Electron Microscopy in Materials Science, Pub: Philips Electronic Instruments, Inc. (1984).

8. B. N. Leis, and T. P. Forte, ASTM STP 743, R. Roberts, ed., Philadelphia, p. 100 (1981).

9. M. H. El Haddad, K. N. Smith and T. H. Topper, ASTM STP 677, C. W. Smith, ed., Philadelphia, p. 274 (1978).

10. A. J. McEvily and K. Minakawa, K., Fatigue Crack Growth Threshold Concepts, AIME Symp. Proc., D. L. Davidson and S. Suresh, eds., Philadelphia, p. 517 (1983).

11. C. W. Brown and D. Taylor, Fatigue Crack Growth Threshold Concepts, AIME Symp. Proc., D. L. Davidson and S. Suresh, eds., Philadelphia, p. 433 (1983).

12. G. P. Sheldon, T. S. Cook, and J. Lankford, Fat. Eng. Mater. Struct. 3, p. 219 (1981).

13. M. E. Fine, J. L. Horng and D. H. Park, Fatigue 84, III, C. J. Beever, ed., England, p. 739 (1984).

14. J. L. Horng and M. E. Fine, Mat. Sci. Eng., 67, p. 185 (1984).

15. S. Suresh, G. F. Zamiski, and R. O. Ritchie, Met. Trans., 12A, p. 1435 (1981).

16. S. Suresh and R. O. Ritchie, Met. Trans. A, 13A, p. 1627 (1982).

17. J. E. King, R. A. Venables and M. A. Hicks, Advances in Fracture Research, 3, p. 2081 (1984).

18. M. A. Hicks and J. E. King, Int. J. Fat., 5(2), p. 67 (1983).

19. B. N. Leis and T. P. Forte, ASTM STP 743, p. 100 (1981).

20. A. J. McEvily and K. Minakawa, Fatigue Crack Growth Threshold Concepts, D. Davidson and S. Suresh, eds., AIME, p. 517 (1984).

21. G. P. Sheldon, T. S. Cook and J. Lankford, Fat. Engrg. Mater. Struct., 3, p. 219 (1981).

22. G. C. Sih and E. Madenci, Eng. Fract. Mech., 18(3), p. 667 (1983).

23. G. C. Sih and C. K. Chao, J. Theor. Appl. Fract. Mech., 2(1), p. 67 (1984).

24. R. Badaliance, Eng. Fract. Mech., 13, p. 657 (1980).

25. W. Elber, Eng. Fract. Mech., 2, p. 37 (1970).

26. W. Elber, ASTM STP 486, p. 230 (1971).

27. S. Suresh, Met. Trans. A, 14A, p. 2375 (1983).

28. R. J. Stofanak, R. W. Hertzberg, G. Miller, R. Jaccard and K. Donald, Eng. Fract. Mech., 17(6), p. 527 (1983).

29. G. T. Gray, J. C. Williams and A. W. Thompson, Met. Trans. 14A, p. 421 (1983).

30. J. L. Horng and M. E. Fine, Mat. Sci. Eng., 67, p. 185 (1984).

31. R. S. Vecchio, J. S. Crompton and R. W. Hertzberg, Int. J. Fract., in press.

32. R. W. Hertzberg and C. H. Newton, ASTM, in review.

33. R. S. Vecchio, R. W. Hertzberg and R. Jaccard, Scripta Met., 17, p. 343 (1983).

34. R. S. Vecchio, R. W. Hertzberg and R. Jaccard, Fat. Eng. Mat. Struct., 7, p. 181 (1983).

35. C. H. Newton, R. S. Vecchio, R. W. Hertzberg and R. Jaccard, Fatigue Crack Growth Threshold Concepts, D. C. Davidson and S. Suresh, eds., p. 379 (1984).

Publications

1. R. S. Vecchio, J. S. Crompton and R. W. Hertzberg, "Fatigue Threshold Behavior in a Nickel Base Superalloy," Fatigue 84, III, C. J. Beevers, ed., Birmingham, England, p. 1379 (1984).

2. R. S. Vecchio and R. W. Hertzberg, "A Rationale for the 'Apparent Anomalous' Growth Behavior of Short Fatigue Cracks," Eng. Fract. Mech., 22 (6), p. 1049 (1985).

3. R. S. Vecchio, D. A. Jablonski, B. H. Lee, R. W. Hertzberg, C. N. Newton, R. Roberts, G. Chen and G. Connelly, "Development of an Automated Fatigue Crack Propagation Test System," ASTM STP 877, p. 44 (1985).

4. D. A. Jablonski, B. Cournet, R. S. Vecchio and R. W. Hertzberg, "Compliance Functions for Various Fracture Mechanics Specimens," Eng. Fract. Mech., 22(5), p. 819 (1985).

5. J. S. Crompton and R. W. Hertzberg, "Analysis of Second Phase Particles in a Powder Metallurgy HIP'd Nickel-Base Superalloy," J. Mater. Sci., in press.

6. R. S. Vecchio, J. S. Crompton and R. W. Hertzberg, "Anomalous Aspects of Crack Closure," Int. J. Fract., in press.

7. R. W. Hertzberg, "Fracture Surface Micromorphology in Engineering Solids," ASTM, in press.

8. R. S. Vecchio, J. S. Crompton and R. W. Hertzberg, "The Influences of Specimen Geometry on Near Threshold Fatigue Crack Growth," Fat. Fract. Eng. Mater. Struct., in review.

9. R. W. Hertzberg and C. N. Newton, "Crack Closure-Correlations and Confusions," ASTM, in review.

10. R. S. Vecchio, "Application of Fracture Mechanics Principles to Fatigue Crack Growth in a Powder Metallurgy Ni-Base Superalloy," Ph.D. Dissertation, Lehigh University 1985.

Personnel

1. Richard W. Hertzberg, Principal Investigator
2. Jeffrey S. Crompton, Research Associate
3. Crystal H. Newton, Research Associate
4. Robert S. Vecchio, Research Assistant

Degree Awarded

Robert S. Vecchio, Ph.D., June 1985
"Application of Fracture Mechanics Principles to Fatigue Crack Growth in a Powder Metallurgy Ni-Base Superalloy."

Interactions

1. Manuscript 1 presented at Fatigue 84 Conference, Birmingham, England, 1984.
2. Manuscript 2 presented at AIME Annual Meeting Spring 1985, New York, NY.
3. Manuscript 3 presented at ASTM Conference, Fall, 1983, Pittsburgh, PA.
4. Manuscript 5 presented at AIME Annual Meeting Spring 1985, New York, NY.
5. Manuscript 7 presented at ASTM Conference Fall 1985, Nashville, TN.
6. Manuscript 9 presented at ASTM Conference Spring 1986, Charleston, SC.
7. Technical discussions on fatigue of nickel-base alloys with Dr. Ted Nicholas, AFWAL/MLLM, Fall 1983. Lecture given by Dr. Nicholas.
8. Technical discussions on fatigue of turbine disks with Dr. Robert Van Stone, G.E. Corp., Evandale, Ohio, Spring 1983. Lecture given by Dr. Van Stone.
9. Technical discussions on short crack growth in nickel-based alloys with Dr. Richard Gangloff, Exxon Corp., Linden, NJ. Lecture given by Dr. Gangloff.
10. Technical discussions on metallurgical aspects of fatigue crack propagation in engineering alloys with Dr. George Yoder, NRL, Washington, DC. Lecture given by Dr. Yoder.

SECURITY CLASSIFICATION OF THIS PAGE

REPORT DOCUMENTATION PAGE

1a. REPORT SECURITY CLASSIFICATION Unclassified	1b. RESTRICTIVE MARKINGS
2a. SECURITY CLASSIFICATION AUTHORITY	3. DISTRIBUTION/AVAILABILITY OF REPORT Approved for public release; distribution unlimited.
2b. DECLASSIFICATION/DOWNGRADING SCHEDULE	
4. PERFORMING ORGANIZATION REPORT NUMBER(S)	5. MONITORING ORGANIZATION REPORT NUMBER(S) **AFOSR-TR- 86-0920**
6a. NAME OF PERFORMING ORGANIZATION Dept. of Metallurgy and Materials Engineering 6b. OFFICE SYMBOL (If applicable)	7a. NAME OF MONITORING ORGANIZATION Air Force Office of Scientific Research
6c. ADDRESS (City, State and ZIP Code) Whitaker Laboratory, Bldg. #5 Bethlehem, Penna. 18015	7b. ADDRESS (City, State and ZIP Code) Building 410 Bolling AFB, Washington DC 20332
8a. NAME OF FUNDING/SPONSORING ORGANIZATION AFOSR /NE 8b. OFFICE SYMBOL (If applicable) NE	9. PROCUREMENT INSTRUMENT IDENTIFICATION NUMBER AFOSR-83-0029
8c. ADDRESS (City, State and ZIP Code) Bolling AFB Washington, DC 20332	10. SOURCE OF FUNDING NOS. PROGRAM ELEMENT NO. 61102F; PROJECT NO. 2306; TASK NO. ~~2306~~/A1; WORK UNIT NO.
11. TITLE (Include Security Classification) A Study of Fatigue Crack Propagation in Powder Metallurgy Hot Isostatically Pressed Nickel-Base Alloy	
12. PERSONAL AUTHOR(S) Hertzberg, Richard Warren	
13a. TYPE OF REPORT Final 13b. TIME COVERED FROM 010183 TO 300686	14. DATE OF REPORT (Yr., Mo., Day) 8/28/86 15. PAGE COUNT 29
16. SUPPLEMENTARY NOTATION	
17. COSATI CODES FIELD / GROUP / SUB. GR.	18. SUBJECT TERMS (Continue on reverse if necessary and identify by block number) Fatigue crack propagation, nickel-based superalloys, powder metallurgy, HIP, grain size influence

19. ABSTRACT (Continue on reverse if necessary and identify by block number)

L.C. Astroloy contains a complex distribution of rounded cuboidal γ' precipitates (0.1 μm edge dimension), cooling γ' (0.01 μm dia) and prior particle boundary particles of MC, ZrO_2, α-Al_2O_3 and M_3B_2; the majority of MC carbides were not found in conjunction with ZrO_2 particles as was previously assumed.

ΔK_{th} values were found to vary with specimen geometry with lower values being associated with more symmetrical specimen geometries. With four-point bend samples, ΔK_{th} increased with increasing grain size, in agreement with previous findings.

The present work has identified several anomalies which exist with respect to crack closure measurements and their correlation of FCP rates. Closure values differed markedly in repeated K-decreasing threshold determinations even though fatigue crack growth rates remained unchanged. The introduction of an artificial asperity in the wake of the crack tip

20. DISTRIBUTION/AVAILABILITY OF ABSTRACT UNCLASSIFIED/UNLIMITED ☒ SAME AS RPT. ☐ DTIC USERS ☐	21. ABSTRACT SECURITY CLASSIFICATION Unclassified
22a. NAME OF RESPONSIBLE INDIVIDUAL Dr. Alan H. Rosenstein	22b. TELEPHONE NUMBER (Include Area Code) 202-767-4931 22c. OFFICE SYMBOL NE

DD FORM 1473, 83 APR EDITION OF 1 JAN 73 IS OBSOLETE.

SECURITY CLASSIFICATION OF THIS PAGE

block 19 cont.

in a 2024 aluminum alloy gave rise to large measured values of closure which had little influence on the crack growth rates; apparently, crack closure had little influence on associated crack growth rates.

Based on experimental and analytical work LEFM principles break down in the "so-called anomalous" short crack regime at relatively high σ/σ_{ys} ratios (e.g., $\sigma/\sigma_{ys} > 0.5$). For example, a fractographic analysis of both long and short crack length specimens revealed different micromechanisms and dissimilar development of shear lips at the same computed ΔK levels. Analytical results also indicated that correlation of short crack data in terms of ΔK is suspect since the near field crack tip stress-strain fields do not possess the required $1/\sqrt{r}$ singularity necessary for the application of LEFM. Short crack data only appear anomalous when plotted in terms of ΔK. However, when short crack and long crack data are analyzed in terms of the strain energy density criterion, excellent agreement is obtained. In addition, this driving force parameter can also account for mean stress effects and rationalize differences in the macroscopic and microscopic fractographic features of long and short cracks.

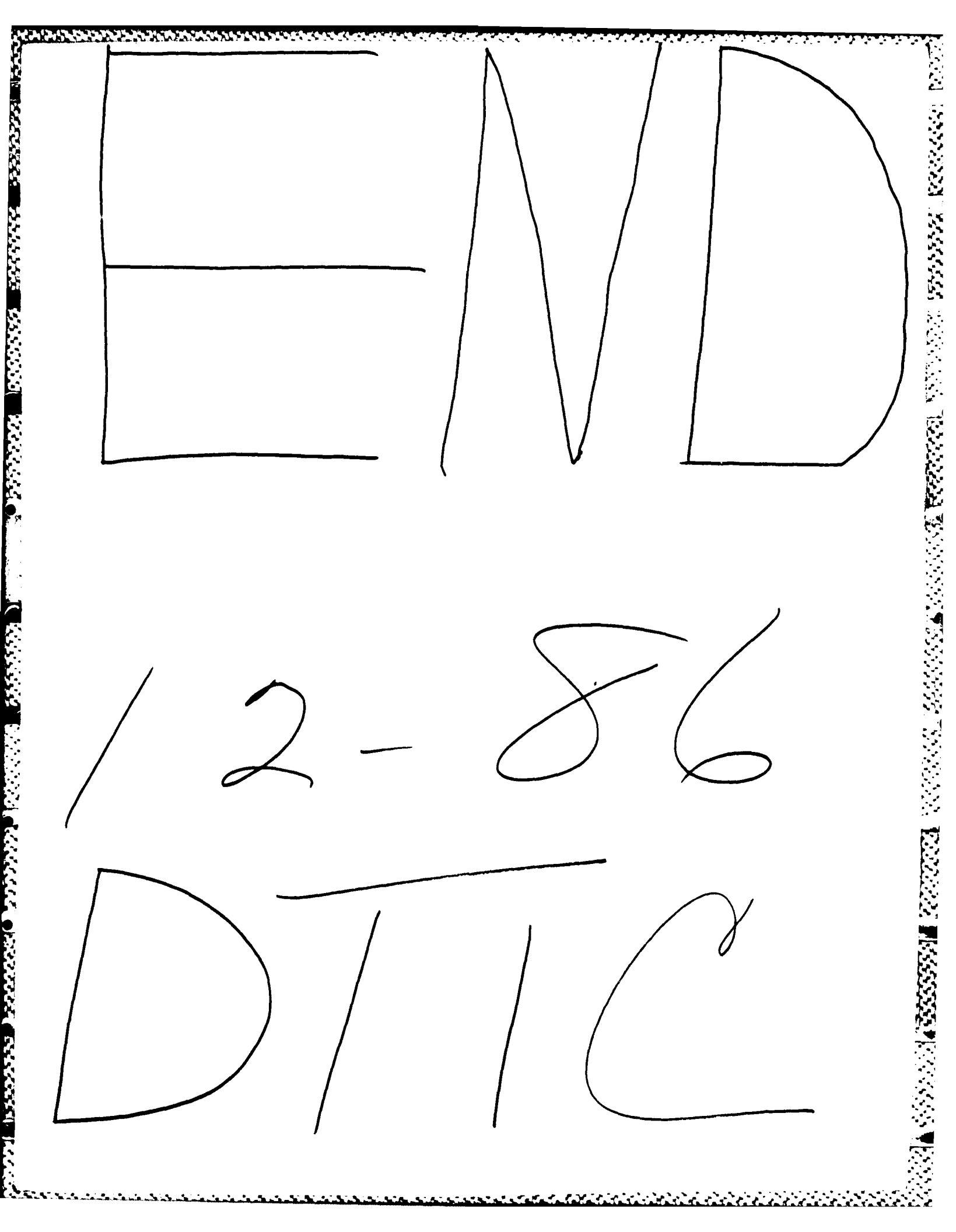
END
12-86
DTIC